engineering proceedings

MDPI

Proceedings

Design of a Characterisation Environment for a MEMS Ultrasound Sensor under Guided Ultrasonic Wave Excitation †

Liv Rittmeier [1,*], Thomas Roloff [1], Jan Niklas Haus [2], Andreas Dietzel [2] and Michael Sinapius [1]

1 Institute of Mechanics and Adaptronics, Technische Universität Braunschweig; e-mail@e-mail1.com (T.R.); e-mail@e-mail2.com (M.S.)
2 Institute of Microtechnology, Technische Universität Braunschweig; e-mail@e-mail3.com (J.N.H.); e-mail@e-mail4.com (A.D.)
* Correspondence: l.rittmeier@tu-braunschweig.de; Tel.: +49-531-391-2682
† Presented at the 8th International Electronic Conference on Sensors and Applications, 1–15 November 2021; Available online: https://ecsa-8.sciforum.net.

Abstract: Micro-Electro-Mechanical Systems (MEMS) are a current subject of research in the field of Structural Health Monitoring (SHM) for the detection of Guided Ultrasonic Waves (GUW). The dispersive behavior of GUW, reflections and other kinds of wave interactions, might result in a complex wave field which requires a specific analysis and interpretation of the recorded signals. This makes it difficult or impossible to interpret the sensor signal regarding the distinguishability between the sensor transfer behavior and the specific behavior of the test structure. Therefore, a proper application-suited design of the tested structure is crucial for reliable sensor characterisation. The aim of this contribution is the design and evaluation of a setup that allows a representative situation for a GUW application and provides a defined vibration energy for a MEMS sensor characterisation. Parameters as the specimen's geometry, material properties and the sensor specifications, are taken into account as well as the experimental settings of the GUW excitation. Furthermore the requirements for the test application case are discussed.

Keywords: Guided Ultrasonic Waves (GUW); Micro-Electro-Mechanical System; test bed; structural dynamics

Citation: Rittmeier, L.; Roloff, T.; Haus, J. N.; Dietzel, A.; Sinapius, M. Design of a Characterisation Environment for a MEMS Ultrasound Sensor under Guided Ultrasonic Wave Excitation. *Eng. Proc.* **2021**, *1*, 0. https://doi.org/

Academic Editor:

Published: 1 November 2021

1. Introduction

Micromechatronic vibration sensors are spring-mass-system based sensors that show a frequency dependent transfer behavior due to resonance effects. The maximum operation frequency of such a sensor depends on the tolerable linearity error. Typically the maximum operation frequency is one order of magnitude below the first resonant frequency ω_0 of the involved spring-mass-system. At frequencies below the resonance frequency, these sensors show nearly linear transfer behaviour between displacement and acceleration [1]. Vibration sensors for frequencies $f < 10$ kHz are typically calibrated using either an impulse or a shaker with a continuous harmonic excitation in combination with a reference transducer [2]. Current research investigates spring-mass system based sensors for dynamic displacements ($f > 100$ kHz), which are operated *quasi-free* ($\omega_{excitation} \gg \omega_{0,sensor}$) [3]. Due to their dynamic behavior, these sensors cannot be used for the acquisition of continuous signals, but can serve to resolve sinusoidal burst signals, as GUW used for SHM.
For ultrasonic signals, the common calibration approaches are not applicable since reference transducers are not available for the high frequency. To however calibrate the sensor for typical GUW signals, a setup can be used, which generates a well-defined waveform at the sensor location. The sensor can then be calibrated on the basis of the known excitement.

The aim of this work is the creation of a test bed for a MEMS sensor under structure-borne GUW excitation and addresses three challenges.

Firstly, material damping has an influence on the possible propagation path length of GUW. Since the particle velocity increases with frequency, the absorption effect increases linear to the frequency. This causes stronger damping effects for higher frequencies [4] (p. 20).

Secondly, GUW show frequency-dependent dispersive behaviour. When excited by a windowed sinusoidal burst signal, the wave packages distort in the course of wave propagation and show a different appearance in the wave field depending on the excitation signal's bandwidth [5]. Also, the regarded frequency range of a considered wave mode might show differently strong dispersive behaviour.

Thirdly, the structure's size causes reflections from the edges due to high propagation velocities. The reflections superpose with the propagating waves and increase the complexity of the wave field. The distinction between the sensor's structural behaviour and the forced vibration from the surrounding environment is crucial for a reliable characterisation process.

2. Materials and Methods

The ultrasound sensor, as presented in [3], is supposed to be operated *quasi-free* in the frequency range from approx. 50 kHz–200 kHz. In reference to the challenges introduced in Section 1, structural and dynamical parameters like material damping, chosen excitation GUW mode and the test bed thickness and size are discussed.

2.1. Material and GUW Mode Selection

The authors choose rolled sheet aluminium as material for the test bed due to lower material damping compared to epoxy resin used in fibre-reinforced polymers [6] (p. 116). This ensures a high range of wave propagation inside the waveguide.

The MEMS sensor will be designed as an out-of-plane vibration sensor. To generate a high signal-to-noise ratio, a sufficiently high out-of-plane component for the sensors' excitation is required. Therefore, the $A0$-mode is selected for the excitation due to its higher out-of-plane component compared to the $S0$-mode [7] (p. 103).

The damping behaviour of the MEMS pickup needs to be identified. The authors' aim is to generate the longest possible time span between the excited fundamental wave modes. This ensures that the excited MEMS sensor's oscillation is declined before an excitation by a following wave package occurs.

2.2. Influence of the Structure's Thickness on the Degree of Dispersion

The authors perform a parameter study on the influence of the aluminium structure's thickness on the degree of dispersion of the A_0-mode. The dispersion relation for an aluminium plate is estimated for three different thicknesses (0.5 mm, 1 mm and 5 mm). The free software GUIGUW is used to solve the dispersion relation which leads to the solution of the frequency-dependent phase velocities, group velocities, wave numbers and wavelengths. The material parameters chosen for the simulation are listed in Table 1.

The group velocity describes the propagation velocity of a wave package. In case of dispersive waves, it differs from the velocities of individual waves in the packages due to the different propagation speeds at different excitation frequencies. The degree of dispersion depends on the time span of the excitation signal i. e. the number of cycles in the burst excitation. It decreases with an increase of cycles in the excitation burst since the excitation spectrum gets narrower and therefore excites less individual waves [5] (p. 154).

The phase velocities in the range of 50 kHz–200 kHz are extracted and derived according to the frequency to quantify the degree of dispersion. From this, the authors can deduce a possible plate thickness that shows the lowest degree of dispersion regarding the $A0$-mode.

Table 1. Material parameters for aluminium used in the GUIGUW-simulation.

Young's Modulus [GPa]	Density [kg m^{-3}]	poisson's ratio [-]
70	2780	0.33

2.3. Estimation of Wave Propagation Behaviour Regarding Mode Separation

A 800 mm × 800 mm wide aluminium plate of 1 mm thickness is used as specimen. Sealant is glued to the edges all around the plate to minimise edge reflections. A round PZT-actuator is applied in the center of the plate. As excitation signal, a 5-cycle Hanning-windowed sinusoidal burst of approx. 1.35 V is chosen which is amplified 40 times by a power amplifier. Two burst center frequencies are chosen: 50 kHz and 200 kHz as limiting cases for the considered frequency range. The time between two burst pulses is 50 ms to avoid superpositions with previously excited reflections. A Laser-Doppler-Vibrometer (LDV) from Polytec GmbH is used for recording the out-of-plane component of the wave field. 17 measurement points are aligned on the aluminium plate's surface. The first measuring point is located approx. 13 mm away from the actuator's centre. All the following points are at an equidistant distance of 22 mm from each other. For the measurement, the aluminium plate is leaned against a fixation which causes an angle between the laser beam and the specimen's surface. The angle correction function of Polytec in x- and y-direction is used to estimate the actual out-of-plane amplitude. A trigonometric compensation calculation is used to compensate angle errors due to a not-perpendicular impact of the laser beam on the plate's surface. The signal is averaged 50 times. The displacement decoder is used to gain information about the absolute deflection amplitude of the structure's surface as a measure of the later sensor excitation amplitude. No digital filtering of the LDV signal is used. The measurement time is set to 400 µs. The measurement is triggered by a system internal trigger signal. For each measuring point, the time signal is examined for occurring modes, mode separation and possible reflections.

3. Results

In this section, the authors deduce the degree of dispersion from the phase velocities as well as the wave propagation behaviour regarding the mode separation of $S0$- and $A0$-mode obtained from an experimental setup. Criteria for the test bed preparation can be deduced regarding the requirements described in Section 2.

3.1. Influence of the Structure's Thickness on the Degree of Dispersion

Based on the different phase velocities for three different aluminium plate thicknesses, the authors deduced the changing rate of the phase velocities of the $A0$-mode as a measure of the degree of dispersion. It leads to the overview as shown in Figure 1.

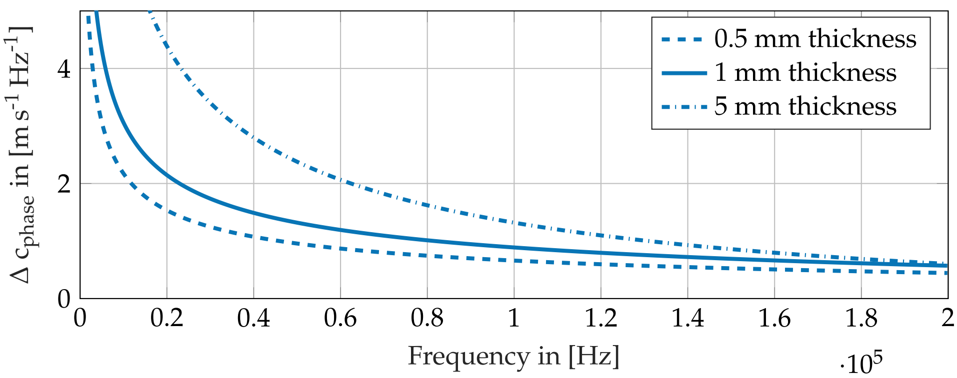

Figure 1. Derivatives of phase velocities (A0-mode in aluminium).

Regarding the frequency range of interest which has already been described in Section 2, the highest phase velocity changing rates are to be expected in the lower frequencies and increase with the plate thickness. With increasing frequency, the phase velocity changing rates approach each other for all plate thicknesses. The authors conclude that, especially for lower frequencies, a thin plate should be chosen over a thicker plate. Therefore a 1 mm aluminium plate is used as a compromise between phase velocity changing rates and experimental manageability.

Figure 2 shows the dispersion diagram of the phase velocity of the two fundamental Lamb wave modes for the selected material. The phase velocity for the $S0$-mode is nearly constant for the regarded frequency range while the phase velocity of the $A0$-mode increases. From 50 kHz to 200 kHz, the phase velocity has approx. doubled.

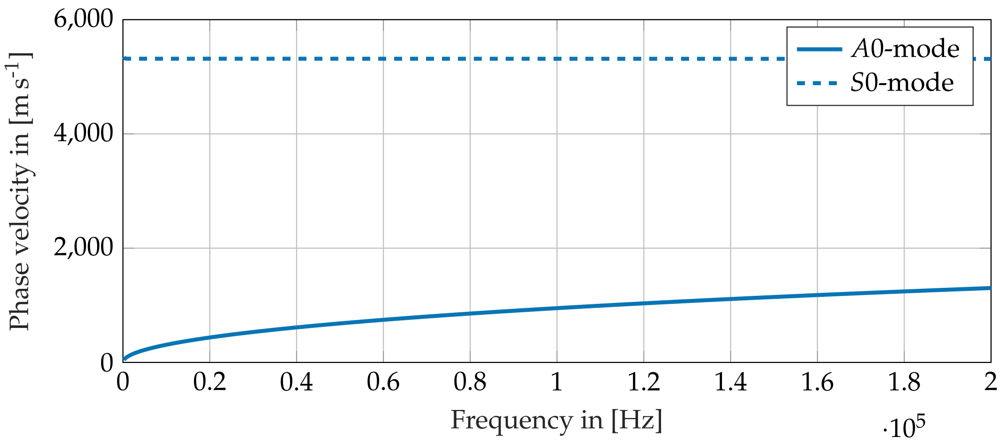

Figure 2. Dispersion Diagram of a 1 mm-thick aluminium plate.

3.2. Estimation of Wave Propagation Behaviour Regarding Mode Separation

In this subsection, it is estimated how mode separation at the two different frequencies occur. For the purpose of sensor characterisation, it is desirable to separate the preferred A_0-mode from the neglected S_0-mode in the time domain, to avoid returning edge reflections due to narrow specimen width dimensions.

Referring to the dispersion relation for a 1 mm-thick aluminium plate of 800 mm × 800 mm width, the S_0-mode will reflect at the edges of the specimen after 75 µs for all excitation frequencies in the considered frequency range. The A_0-mode at 200 kHz will start to reflect after 300 µs and at 50 kHz it will reflect after 580 µs due to the higher degree of dispersion in this frequency range as can be seen from Figure 1. Therefore the authors expect a S_0-mode reflection during the selected measurement time for wave propagation in the considered frequency range.

For this estimation, the time difference between the maximum of the excitation burst and the maximum of the considered wave package was assumed.

3.2.1. Mode Separation at 50 kHz

Figure 3 shows the wave propagation at two selected points for a burst center frequency of 50 kHz. The mode separation starts to be visible at approx. 123 mm running length as shown in Figure 3a. In the following course along the path the $S0$-mode shows a very low-amplitude in comparison to the $A0$-mode .

In Figure 3b the modes are separated. Along the following measurement path to the plate's edge, it can not be clearly said if a $S0$-reflection starts to be visible as a returning wave. Referring to the estimation of the reflection times described in Section 3.2, a reflected S_0-mode should occur.

3.2.2. Mode Separation at 200 kHz

At 200 kHz at a distance of approx. 123 mm from the actuator, the $S0$-mode and the $A0$-mode start to separate due to their different propagation speeds as visible in Figure 4a. Following the path the modes separate more in time. At a distance of approx. 300 mm from the actuator, another mode separates from the $A0$-mode which the authors identify as an edge reflection of the $S0$-mode. Figure 4b shows the three occuring wave packages: The forward propagating $S0$-mode and the forward propagating $A0$-mode after their separation and the reflected $S0$-mode. In the course of the path this reflection starts to superpose with the forward-running $S0$-mode at a distance of approx. 350 mm.

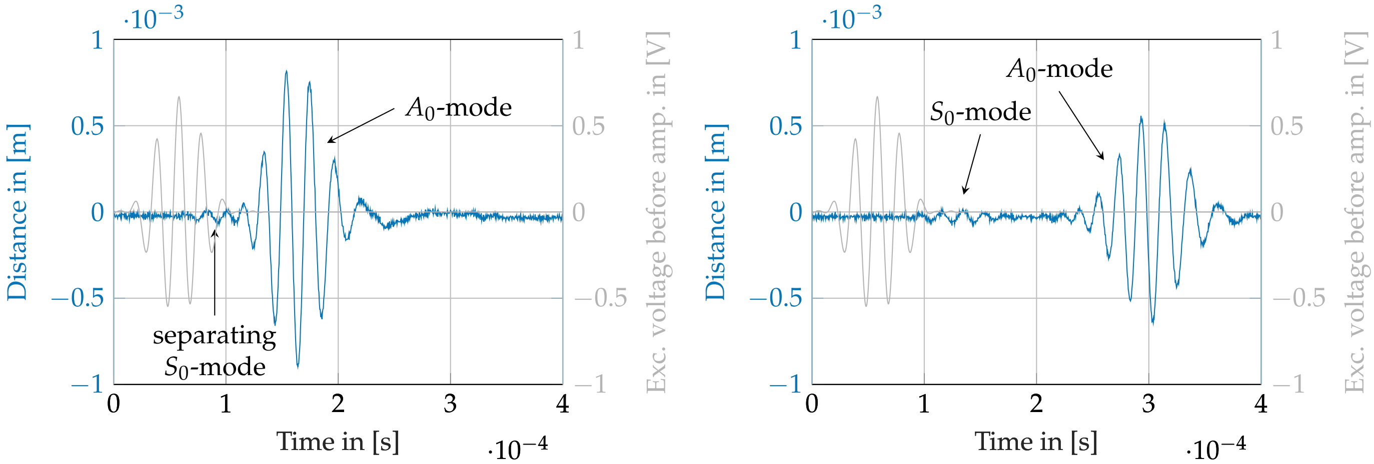

(**a**) Separating wave modes at approx. 123 mm (**b**) Fully separated waves modes at approx. 303 mm

Figure 3. Wave propagation at 50 kHz.

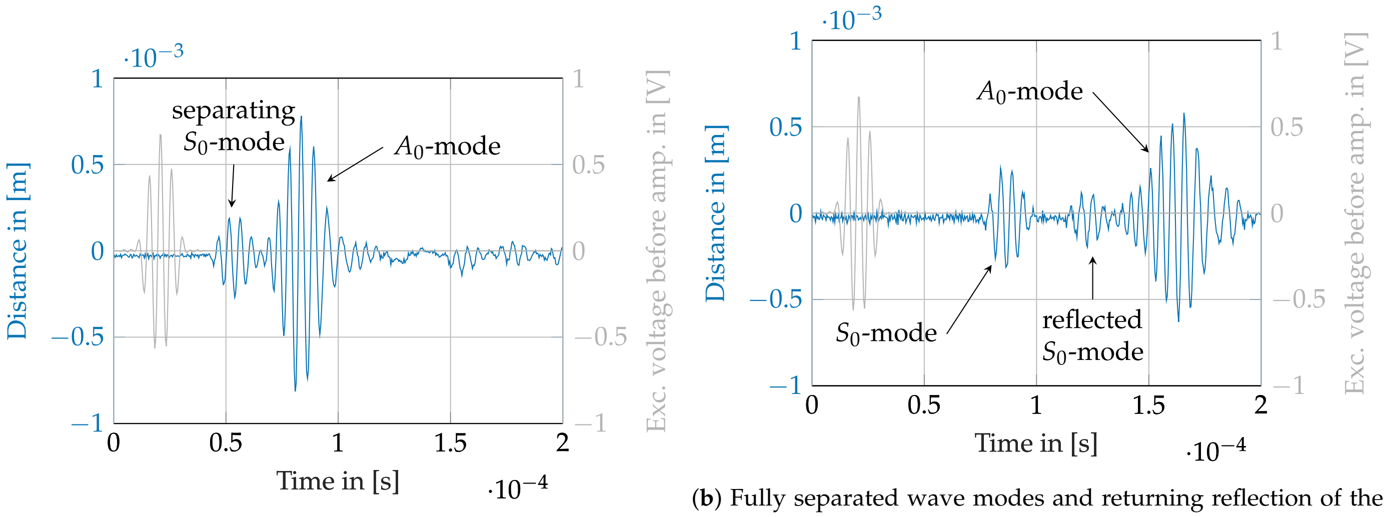

(**a**) Separating wave modes at approx. 123 mm

(**b**) Fully separated wave modes and returning reflection of the $S0$-mode at approx. 303 mm

Figure 4. Wave propagation at 200 kHz.

4. Discussion

The experimental study shows that edge reflections make it difficult to clearly separate the wave modes as defined input excitation signals for a later sensor calibration test bed. The authors conclude, that mode selective excitation as well as a good damping at the specimen's edges is required to be able to use a specimen of a limited width. Additionally, the structure's dispersive behaviour should be taken into account. Ideally, the sensor characterisation is performed in a frequency range with low dispersion or dependent on the desired frequencies on a structure that shows a low degree of dispersion in the considered frequency range.

At 200 kHz, due to the edge reflection of the $S0$-mode, it was not possible with the used plate specimen to gain separated modes with sufficiently long time separation because the edge reflection started to superpose shortly after the separation of the $A0$-mode and $S0$-mode took place.

At a position of approx. 303 mm running length, the comparison between the times of flight of the A_0-mode show, that it doubles at 50 kHz in comparison to 200 kHz. This can be explained by the doubling of the phase velocity of the A_0-mode at 200 kHz (approx. 1300 ms^{-1}) in comparison to it's phase velocity at 50 kHz (approx. 690 ms^{-1}) as shown in Figure 2.

5. Conclusions

The authors conclude that for a test bed a possibly thin aluminium plate should be used which is as wide as possible in its' width dimensions. This helps prevent edge reflections. Additionally, $S0$-mode reflections can be suppressed in the first place when a mode-selective excitation for the $A0$-mode is realized which minimises the $S0$-mode excitation. Referring to the evaluated distances in our setup at which mode separation starts to occur, no distances less than 300 mm to the actuator in the plate's center should be chosen for acceleration sensor positioning. The complete mode separation at both evaluated frequencies has taken place after 300 mm of measurement path. In a wider aluminium plate, it can be assumed that the separated modes have sufficient time span between each other so that the oscillation of an applied sensor excited by the A_0-mode can be observed. Further forced excitation by reflected waves can be avoided.

The authors conclude that an adjusted setup can be realized under consideration of the requirements for sensor calibration.

Funding: The authors expressly acknowledge the financial support of the research work on this article within the Research Unit 3022 "Ultrasonic Monitoring of Fibre Metal Laminates Using Integrated Sensors" (Project number: 418311604) by the German Research Foundation (Deutsche Forschungsgemeinschaft (DFG)).

Institutional Review Board Statement:

Informed Consent Statement:

Data Availability Statement: The raw data of the experiments can be requested from the authors.

Conflicts of Interest: The authors declare no conflict of interest. The funders had no role in the design of the study; in the collection, analyses, or interpretation of data; in the writing of the manuscript, or in the decision to publish the results.

References

1. Büttgenbach, S.; Constantinou, I.; Dietzel, A. (Eds.) *Case Studies in Micromechatronics: From Systems to Processes*, 1st ed. 2020 ed.; 2020.
2. Veldman, C.S. ISO 16063; A comprehensive set of vibration and shock calibration standards. In Proceedings of the XVIII IMEKO World Congress Metrology for a Sustainable Development, Citeseer, Rio de Janeiro, Brazil, 17–22 September 2006; pp. 1–5.
3. Haus, J.N. *MEMS Ultrasound Sensor with Functional Compliance for Structural Health Monitoring in Fiber Metal Laminates*; Poster Presented at MNE 2021; Turin, Italy, 2021.
4. Nico Liebers. Ultraschallsensorgeführte Infusions- und Aushärteprozesse für Faserverbundkunststoffe. Dissertation, DLR, 2018.
5. Giurgiutiu, V. *Structural Health Monitoring with Piezoelectric Wafer Active Sensors*; Academic Press/Elsevier: Amsterdam, The Netherlands, 2008.
6. Krautkrämer, J.; Krautkrämer, H. (Eds.) *Werkstoffprüfung Mit Ultraschall*; 3., neubearb. aufl./unter mitarb. von ed.; Springer: Berlin/Heidelberg, Germany, 1975.
7. Gabbert, U.; Sinapius, M.; Schuster, T.; Wierach, P.; Lammering, R. *Lamb-Wave Based Structural Health Monitoring in Polymer Composites*, 1st ed. 2017 ed.; Lehrbuch; Springer International PU [S.l.]: 2017.